# Principle of Locality and Analysis of Radio Occultation Data

Alexander G. Pavelyev, Kefei Zhang, Yuei-An Liou, *Senior Member, IEEE*, Alexey A. Pavelyev, Chuan-Sheng Wang, Jens Wickert, Torsten Schmidt, and Yuriy Kuleshov

***Abstract*—A fundamental principle of local interaction of radio waves with a refractive spherical medium is formulated and illustrated using the radio occultation (RO) method of remote sensing of the atmosphere and the ionosphere of the Earth and the planets. In accordance with this principle, the main contribution to variations of the amplitude and the phase of radio waves propagating through a medium makes a neighborhood of a tangential point, where the gradient of the refractive index is perpendicular to the radio wave trajectory. A necessary and sufficient condition (a criterion) is established to detect the displacement of the tangential point from the radio ray perigee using analysis of the RO experimental data. This criterion is applied to the identification and the location of layers in the atmosphere and the ionosphere by the use of Global Positioning System RO data. RO data from the CHAllenge Minisatellite Payload (CHAMP) are used to validate the criterion introduced when significant variations of the amplitude and the phase of the RO signals are observed at the RO ray perigee altitudes below 80 km. The detected criterion opens a new avenue in terms of measuring the altitude and the slope of the atmospheric and ionospheric layers. This is important for the location determination of the wind shear and the direction of internal wave propagation in the lower ionosphere and possibly in the atmosphere. The new criterion provides an improved estimation of the altitude and the location of the ionospheric plasma layers compared with the backpropagation radio-holographic method previously used.**

***Index Terms*—Bistatic remote sensing, geophysical signal processing, global positioning system, occultations, radio wave propagation, terrestrial and planetary atmospheres and ionospheres.**

Manuscript received October 28, 2011; revised May 24, 2012 and October 3, 2012; accepted October 7, 2012. Date of publication January 21, 2013; date of current version May 16, 2013. This work was supported in part by the National Science Council and the National Space Organization of Taiwan, under Grants NSC 101-2111-M-008-018 and 101-2221-E-008-019, by the Russian Fund of Basic Research under Grant 10-02-01015-a, by Program 22 of the Russian Academy of Sciences, by Australian Research Council Project ARC-LP0883288, by the Department of Industry, Innovation, Science, and Research of Australia International Science Linkage under Project DIISR/ISL-CG130127, and by the Australia Space Research Program Project endorsed to research consortiums led by the Royal Melbourne Institute of Technology University.

A. G. Pavelyev and A. A. Pavelyev are with the Kotelnikov Institute of Radio Engineering and Electronics, Russian Academy of Sciences, Moscow 141120, Russia (e-mail: alxndr38@mail.ru).

K. Zhang is with the School of Mathematical and Geospatial Sciences, Royal Melbourne Institute of Technology University, Melbourne, Vic 3001, Australia.

Y.-A. Liou is with the Center for Space and Remote Sensing Research, National Central University, Chung-Li 320, Taiwan.

C.-S. Wang is with the National Taipei University, New Taipei City 23741, Taiwan.

J. Wickert and T. Schmidt are with the GeoForschungsZentrum (GFZ), Potsdam 14473, Germany.

Y. Kuleshov is with the National Climate Centre, Bureau of Meteorology, Melbourne, Vic 3001, Australia.

Digital Object Identifier 10.1109/TGRS.2012.2225629

## I. Introduction

THE radio occultation (RO) method employs the highly stable radio waves transmitted at two GPS frequencies $f_1 = 1575.42$ MHz and $f_2 = 1227.60$ MHz by the GPS satellites and recorded at a GPS receiver onboard a low Earth orbiting (LEO) satellite to remotely sense the Earth's ionosphere and neutral atmosphere [1]–[26]. When applied to ionospheric investigations, the RO method may be considered as a global tool and can be compared with the global Earth- and space-based radio tomography [26], [27]. The RO method delivers a great amount of data on the electron density distribution in the upper and lower ionospheres that are important sources for modernizing the current information over the morphology of the ionospheric processes [28], [29]. The RO method has been actively used to study the global distribution of sporadic $E$-layers in the dependence of latitude, longitude, altitude, and local time [6], [12], [15]–[17], [23]–[25], [30]–[32]. These investigations have produced useful data on climatology and the formation process of sporadic $E$-layers, which mainly depend on the Earth's magnetic field and meteor impact according to the theory of the wind shear mechanism of plasma concentration [13], [33]–[35]. The thermospheric wind and the atmospheric tides seem to be the main energy sources for this mechanism [25].

Therefore, the spatial distributions of sporadic $E$-layers are important for investigating the connections of natural processes in the neutral and ionized components of the ionosphere. The location and the intensity of sporadic $E$-layers play a critical role for the quality of radio communications in the high-frequency band. The RO measurements in the atmosphere can be significantly affected by ionospheric contributions since the RO signals propagate through two different parts of the ionosphere. Usually, the ionospheric influence in the RO measurements may be described through a relatively slow change in the excess phase without noticeable variations in the amplitude of RO signals. This effect can be essentially reduced by a number of different methods of ionospheric correction [36]–[39].

However, the disturbed ionosphere may significantly change not only the phase but also the amplitude of the RO signals. Strong amplitude and phase frequency-dependent variations in the RO signals are often surprisingly observed within the altitudes of the RO ray perigee $h(T)$ between 30 and 80 km above the main part of the neutral atmosphere and below the $E$-layer of the ionosphere. The effects of strong phase and amplitude variations of the RO signals at a low altitude

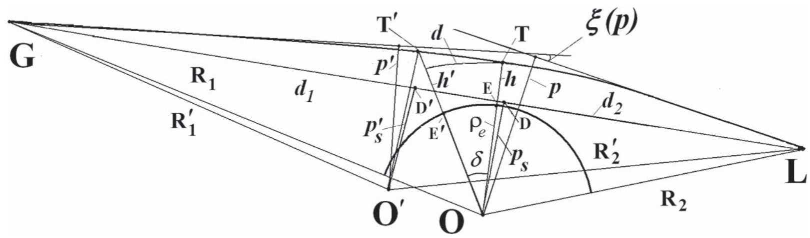


Fig. 1. Geometrical parameters of the RO experiment.

provide a good source of information for the remote sensing of the atmosphere and the ionosphere including detecting and studying the internal gravity waves (GWs) propagating in the atmosphere and the ionosphere [40]. Accurate knowledge of spatial location, height, and inclination of the sporadic $E$-layers is important for the estimation of the off-equatorial height-integrated conductivity [28], [29]. The RO low-altitude amplitude variations have been interpreted as contribution from the inclined ionospheric layers displaced relative to the RO ray perigee and equations have been developed for the determination of the height and the slope of inclined plasma layers from their displacement [6].

The altitudes of sporadic $E$-layers have been evaluated as the height of the RO radio ray perigee in recent times [12], [23]–[25]. The relationship between the eikonal (phase path) and amplitude variations in the GPS Meteorology (GPS/MET) RO data has been analyzed, and the following conclusions have been made: 1) The amplitude variations in distinction to the phase of RO signal have a strong dependence on the distance from observation point to the location of an ionospheric irregularity. 2) The location of the irregularities in the low ionosphere may be determined by measuring the distance between the observation point up to a phase screen, which should be perpendicularly located to the RO ray trajectory at its perigee [41]. A radio-holographic backpropagation method has been suggested and applied for the location of the irregularities in E- and F-layers of the ionosphere [38], [42].

A relationship between the derivatives of the phase, eikonal, and Doppler frequency on time and intensity of radio waves propagating through the near Earth's space has been detected [43] and then validated using both theoretical considerations and experimental analysis of the RO radio holograms. The introduced eikonal acceleration technique can be applied for locating layers in the ionosphere and the atmosphere [15], [16], [21], [22], [30]–[32].

The main aim of this paper is to introduce a locality principle and to demonstrate the possibility of identifying the contributions and measuring parameters of the inclined plasma layers. This paper is structured as follows. In Section II, a locality principle and a criterion rule to detect a layer's contribution to the RO signals are presented, and a method for identification and location of plasma layers is described. In Section III, a test of a suggested method is provided by the use of CHAMP RO data. Conclusions are given in Section IV.

## II. Criterion for Location of Plasma Layers

The scheme of RO experiments is shown in Fig. 1. A navigational satellite $G$ emitted highly stable radio waves, which, after propagation through the ionosphere and the atmosphere along the radio ray $GTL$ arrived to a receiver onboard the LEO satellite $L$. The amplitudes and phase variations of the RO signals are recorded as functions of time, sent to the ground stations with orbital data and analyzed with an aim to find the physical parameters of the neutral atmosphere and ionosphere along the trajectory of the RO radio ray perigee point $T$ (see Fig. 1). The receiver onboard LEO records amplitudes $A_1(t)$ and $A_2(t)$, and the excess phase paths $\Phi_1(t)$ and $\Phi_2(t)$ of the GPS transmitted radio wave signals as a function of time $t$ at two GPS frequencies. The global spherical symmetry of the ionosphere and the atmosphere with a common center of symmetry is the cornerstone assumption of the RO method. Under this assumption, a small area centered at a tangent point $T$ (see Fig. 1), where the RO ray is perpendicular to the gradient of refractivity, makes a significant contribution to the amplitude and phase variations of RO signals despite the prolonged path $GTL$ (see Fig. 1). Under the global spherical symmetry condition, the tangent point coincides with the RO ray perigee $T$. The size of this area along the ray $GTL$ is equal to the horizontal resolution of the RO method $\Delta_h = 2(2l_f\rho_e)^{1/2}$, where $l_f = (\lambda d_2)^{1/2}$ is the size of the Fresnel zone, $\lambda$ is the wavelength, $\rho_e$ is the distance $TO$, $d_2$ is distance $TL$, which is nearly equal to $DL$ (see Fig. 1). The magnitude of $\Delta_h$ corresponds to the minimal horizontal length of a layer estimated by the RO method.

The quiet ionosphere introduces regular trends in the excess phases at two GPS frequencies, which can be removed by the ionospheric correction procedure [39]. The contributions in the phase and amplitude variations of RO signals of the intensive sporadic $E$-layers at the altitude interval of 90–120 km is significantly greater than the impact of the F-layer turbulent structures [3]. The impact of a regular layer on the RO signal depends on the position relative to the RO ray perigee. Length $l_{c\varepsilon}$ of the coherent interaction of the RO signal with a layer having the vertical width $l$ depends on the elevation angle $\varepsilon$ between the local horizontal direction and ray trajectory, i.e., $l_{c\varepsilon} \approx l/\sin\varepsilon$. For the RO ray perigee, the elevation angle $\varepsilon$ is zero, and the corresponding value $l_c$ is described by the following relationship:

$$l_c = 2(2l\rho_e)^{1/2}. \tag{1}$$

Ratio $G$ of lengths $l_c$ and $l_{c\varepsilon}$ is equal to

$$G = \frac{l_c}{l_{c\varepsilon}} = 2\sqrt{\frac{2\rho_e}{l}}\sin\varepsilon. \tag{2}$$

Under the spherical symmetry condition $\sin\varepsilon$ is about 0.25 at the altitude of ionospheric F-layer at 250 km, and one can obtain from (2) the following:

$$G \approx 0.5\sqrt{\frac{2\rho_e}{l}} \approx \frac{0.57 \cdot 10^2}{l^{1/2}}. \tag{3}$$

If the vertical width $l$ is about 1 km, the contribution to the phase variations of a layer disposed in the RO ray perigee differs by about a hundred times on the impact of the similar layer located in the F-region. Therefore, as a rule, the RO method is an effective tool for layer detection and measurements of their parameters with high vertical resolution and accuracy along the trajectory of the RO ray perigee.

The next connection between the excess phase path (eikonal) $\Phi(t)$ acceleration $a$ and the refractive attenuation of electromagnetic waves $X_p(t)$ has been detected and validated [15], [16], [21], [43]

$$1 - X_p(t) = ma,\ a = \frac{d^2\Phi(t)}{dt^2},\ m = d_2(1 - d_2/R_0)/(dp_s/dt)^2 \tag{4}$$

where $d_2$ and $R_0$ are the distances along the straight lines $DL$ and $GL$, respectively, $p$ and $p_s$ are the impact parameters corresponding to ray $GTL$ and the line of sight $GL$ (see Fig. 1). Note that distance $d_2$ is nearly equal to distance $TL$ within an accuracy corresponding to the horizontal resolution of the RO method (about 100–300 km). Parameters $m$ and $dp_s/dt$ may be evaluated from the orbital data. The first formula (4) has been derived under the following condition [21]:

$$\left|(p - p_s)\frac{dR_{1,2}}{dt}\right| \ll \left|p_s\frac{dp_s}{dt}\right| \tag{5}$$

where $R_1$ and $R_2$ are distances $OG$ and $OL$, respectively (see Fig. 1). Condition (5) holds for the RO studies of atmospheres and ionospheres of the Earth and the planets because the module of difference $p - p_s$ is always well below the magnitudes of $p$ and $p_s$. If absorption is absent, magnitude $X_p(t)$ describes the refractive attenuation determined from the amplitude data, i.e.,

$$X_p(t) \equiv X_a(t) \tag{6}$$

$$X_a(t) = I/I_0 \tag{7}$$

where $I_0$ and $I$ are the intensities of the RO signals measured before and after the immersion of the RO ray in the atmosphere, respectively. It should be noted that the total absorption in the atmosphere can be determined by excluding the refractive attenuation found from measurements of the eikonal acceleration at the same frequency by the use of the first equation (4)

$$\Gamma = 1 - X_a(t)/X_p(t). \tag{8}$$

Equations (4) and (8) are the basis of the proposed method for determining the total absorption by measuring the time dependence of the intensity and the eikonal of the RO signal at one frequency [16]. This method is much simpler than the previously used method based on the estimation of the refractive attenuation on the first derivative of the bending angle on the impact parameter.

When the total absorption is absent, it follows from (4) and (6), if the center of symmetry is located at point $O$, i.e.,

$$1 - X_p(t) \equiv 1 - X_a(t) = ma. \tag{9}$$

Relationship (9) establishes the equivalence of values $X_p(t)$ and $X_a(t)$ in the case of the spherical symmetry with center $O$. Identity (9) is a necessary and sufficient condition to ensure that the tangential point coincides with the radio ray perigee. This condition is valid when the total absorption is absent under the requirement of global spherical symmetry. In this case, the locality principle claims that the tangential point coincides with the radio ray perigee if and only if the changes of the refractive attenuations found from the phase and amplitude variations of the RO signal are the same at any time, and that these variations can be attributed to the interaction of the radio wave only with a local small area near the ray perigee. Therefore, the RO method is based on an implicit locality principle, and the RO technology results correspond to the trajectory of motion of the RO ray perigee in the case of a spherically symmetric medium.

The locality principle has a general meaning for the RO technique as applied to the investigation of the planetary ionospheres and atmospheres.

By the use of the locality principle, the theory of the RO method can be extended to develop an appropriate technique for finding locations of the tangent points on the RO ray. This is an aim of the last part of this section.

In some cases, the centers of spherical symmetry in the two parts of the ionosphere located on path $GTL$ (see Fig. 1) do not coincide with that of the neutral atmosphere [16], [17], [30]–[32], [43]. This effect can be caused by the displacement of the center of spherical symmetry $O'$ of the ionospheric part of ray $GTL$ from point $O$ (see Fig. 1). In this case, according to the derivation previously made [21], inequality (5) is also valid after changing distances $R_{1,2}$ to $R'_{1,2}$ and impact parameters $p, p_s$ to $p', p'_s$ because of the smallness of difference $p' - p'_s$ as compared with any of values $p'$ and $p'_s$. Therefore, identity (6) is valid also in the new coordinate system with center at point $O'$ (see Fig. 1), i.e.,

$$X'_p(t) \equiv X_a(t) \tag{10}$$

where $X'_p(t)$ is the new value of the refractive attenuation relevant to a new center of spherical symmetry, i.e.,

$$1 - X'_p(t) = m'a, \quad a = \frac{d^2\phi(t)}{dt^2}$$
$$m' = d'_2\left(1 - d'_2/R_0\right)/\left(dp'_s/dt\right)^2 \tag{11}$$

where $m'$ is a value of parameter $m$ corresponding to center $O'$, and $d'_2$ is distance $D'L$ (see Fig. 1). As compared with formula (4), the first equation (11) is different with new values of the refractive attenuation $X'_p(t)$ and parameter $m'$. The refractive attenuation $X_a(t)$ found from the amplitude data (7) and the eikonal acceleration $a$ does not depend on the location of the spherical symmetry center.

Identity (10) extends criterion (6) to the general case in which the center of spherical symmetry is shifted to an arbitrary point. This allows one to generalize the locality principle for the remote sensing of the stratified spherical medium in the absence of absorption; a certain point of the radio ray is tangential if and only if the refractive attenuations found from the eikonal respective to this point and intensity variations of the radio waves passed through the medium are equal. In this case, both the intensity and the eikonal variations are mainly influenced by a small neighborhood of the tangential point.

The locality principle allows one to determine the location of a tangential point and to find the displacement and then the altitude, and the slope of a layer from the radio ray perigee. According to (4) and (11), it follows

$$1 - X_a(t) \equiv \frac{m'}{m}(1 - X_p) \tag{12}$$

where the refractive attenuation $X_p$ is determined from (4) using the measured value $a$; coefficients $m'$ and $m$ correspond to centers $O'$ and $O$, respectively . It follows from (4), (11), and (12) that

$$X_p - X_a(t) = \left(\frac{m'}{m} - 1\right)(1 - X_p) = \left[\frac{d_2'(1-d_2'/R_0)(dp_s/dt)^2}{d_2(1-d_2/R_0)\,(dp_s'/dt)^2} - 1\right](1 - X_p). \tag{13}$$

If the displacement of the center of spherical symmetry satisfies the following conditions:

$$d_2/R_0, \quad d_2'/R_0 \ll 1; \quad \frac{dp_s}{dt} \approx \frac{dp_s'}{dt} \tag{14}$$

then one can find from (13)

$$X_p - X_a(t) = \frac{d_2' - d_2}{d_2}(1 - X_p) = \frac{d}{d_2}(1 - X_p) \tag{15}$$

where $d$ is distance $DD'$ (see Fig. 1). In the case of the small refraction effect, distance $d$ is approximately equal to the length of arc $TT'$. Relationship (15) establishes a connection between the displacement of the tangential point from the radio ray perigee $d$ and variations of the refractive attenuations $X_a(t)$ and $X_p(t)$.

Let us consider the refractive attenuation variations as the analytical signals in the following form:

$$1 - X_p(t) = ma = A_p(t)\mathrm{Re}\left[\exp j\chi_p(t)\right]$$
$$1 - X_a(t) = A_a(t)\mathrm{Re}\left[\exp j\chi_a(t)\right] \tag{16}$$

where $A_p(t)$ and $A_a(t)$, and $\chi_p(t)$ and $\chi_a(t)$ are correspondingly the amplitudes and the phases of the analytical signals, relevant to functions $1 - X_p(t)$ and $1 - X_a(t)$. Amplitudes and phases $A_p(t)$ and $A_a(t)$, $\chi_p(t)$ and $\chi_a(t)$ describe the atmospheric (ionospheric) modulations of the refractive attenuation variations $1 - X_p(t)$ and $1 - X_a(t)$. Phases $\chi_p(t)$ and $\chi_a(t)$ differ from the excess phase path (eikonal) $\Phi(t)$. In the case when variations $1 - X_p(t)$ and $1 - X_a(t)$ can be described by a narrow-band process, functions $A_{p,a}(t)$ and $\chi_{p,a}(t)$ can be found by the numerical Hilbert transform or by other methods of the digital data analysis.

After substitution (16) in (12), one can obtain

$$A_a(t)\mathrm{Re}\left[\exp j\chi_a(t)\right] \equiv \frac{m'}{m}A_p(t)\mathrm{Re}\left[\exp j\chi_p(t)\right]. \tag{17}$$

Ratio $m'/m$ is supposed to be nearly constant during an RO event. For fulfilling (17), phases $\chi_p(t)$ and $\chi_a(t)$ should be equal, but amplitudes $A_a(t)$ and $A_p(t)$ are different. In this case, one can obtain from (17) under conditions (14) an alternative relationship for displacement $d$, i.e.,

$$d = d_2' - d_2 = d_2\frac{A_a - A_p}{A_p}; \; d_2 = \sqrt{R_2^2 - p_s^2}; \; m' = \frac{A_a}{A_p}m. \tag{18}$$

Equation (18) establishes a rule: the location of a tangent point on the ray trajectory can be fulfilled using the analytical amplitudes of the refractive attenuation variations $A_{a,p}$; displacement $d$ is positive or negative depending on the sign of difference $A_a - A_p$, and the tangent point $T'$ is located on parts $GT$ or $TL$, respectively. Phases $\chi_p(t)$ and $\chi_a(t)$ should be equal within some accuracy determined by a quality of measurements. Note that (18) is valid when the distance of one of the satellites from the ray perigee $T$ is many times greater than the corresponding value for the second one. This condition is fulfilled for the planetary RO experiments provided by the use of the communication radio link spacecraft–Earth and GPS occultations [16].

The correction to the layer height $\Delta h$ and its inclination $\delta$ with respect to the local horizontal direction can be obtained using displacement $d$ [6], i.e.,

$$\delta = d/\rho_e \qquad \Delta h = 0.5 d\delta \tag{19}$$

where $\rho_e$ is distance $TO$ (see Fig. 1).

The condition of the spherical symmetry with new center $O'$ justifies the application of the Abel transform for the solution of the inverse problem. For the Abel transform, the following formula is used [44]:

$$N(p_0) = -\frac{1}{\pi}\int_{p_0}^{\infty} \ln\left[\frac{p}{p_0} + \sqrt{\left(\frac{p}{p_0}\right)^2 - 1}\right]\frac{d\xi(p)}{dp}dp$$
$$\frac{dN(p_0)}{dh} = \frac{1 + N(p_0)}{\left(1 - \frac{dN(p_0)}{dp_0}(r_e + h)\right)}\frac{dN(p_0)}{dp_0} \tag{20}$$

where $p_0$ is the magnitude of the impact parameter $p$ corresponding to ray $GTL$ in the initial instant of time $t_0$, and $N(p_0)$ and $dN(p_0)/dh$ are the refractivity and its vertical gradient. The derivative of the bending angle $\xi(p)$ on the impact parameter $p$ $(d\xi(p)/dp)$ can be found from the refractive attenuation $X$ using an equation previously obtained [45], i.e.,

$$X = \frac{p}{p_s\left|1 - \frac{\sqrt{R_1^2-p^2}\sqrt{R_2^2-p^2}}{R_0}\frac{d\xi}{dp}\right|}$$
$$\frac{d\xi}{dp} \approx \left(1 - \frac{1}{X}\right)\frac{R_0}{\sqrt{R_1^2 - p^2}\sqrt{R_2^2 - p^2}} \tag{21}$$

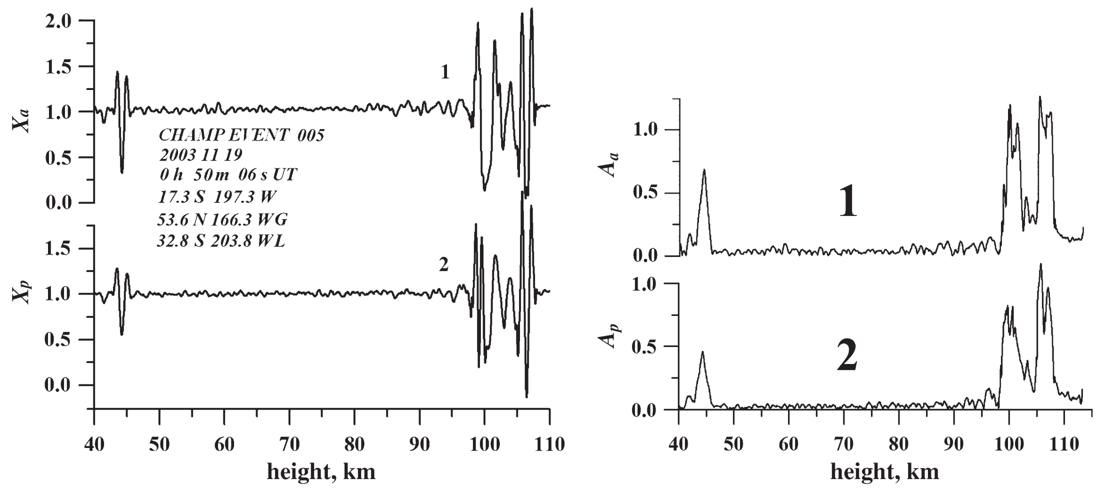


Fig. 2. (Left plot) Refractive attenuations $X_a$ and $X_p$ found from the intensity and eikonal RO data at frequency $f_1$ (curves 1 and 2, respectively). (Right plot) Amplitudes $A_a$ and $A_p$ of analytical signals corresponding to the variations of the refractive attenuations $X_a$ and $X_p$ (curves 1 and 2).

where $R_0$ is distance $GL$ (see Fig. 1). From (4), (20), and (21), one can obtain a modernized formula for the Abel inversion, i.e.,

$$N(p_0) = \frac{1}{\pi} \int_{t_0}^{t_x} \ln \left[ \frac{p(t)}{p_0} + \sqrt{\left(\frac{p(t)}{p_0}\right)^2 - 1} \right] \times \frac{m'a}{\sqrt{R_2^2 - p^2(t)}} \frac{dp_s}{dt} \, dt. \quad (22)$$

Factor $m'$ in (22) can be estimated from the last equation (18). Magnitude $m'a$ in (22) may be changed by value $1 - X_a$ to directly use the RO amplitude data for the Abel inversion. Note that (22) provides the Abel transform in the time domain $t_0$ and $t_x$, where a layer contribution does exist. The linear part of the regular trend due to the influence of the upper ionosphere is removed because the eikonal acceleration $a$ in (22) contains the second derivative on time. However, the influence of the upper ionosphere is existing because it contributes in the impact parameter $p(t)$. Also, the nonlinear contribution of the upper ionosphere remains in the eikonal acceleration $a$. Therefore, (22) approximately gives that part of the refractivity altitude distribution, which is connected with the influence of a sharp plasma layer. The electron density vertical distribution in the Earth's ionosphere $N_e(h)$ is connected at GPS frequencies with the refractivity $N(h)$ via the following relationship:

$$N_e(h) = -\frac{N(h) f^2}{40.3} \quad (23)$$

where $f$ is the carrier frequency [Hz], $N_e(h)$ is the electron content [el/m$^3$].

## III. Analysis of CHAMP Experimental Data

To consider a possibility to locate the plasma layers, we will use a CHAMP RO event 005 (November 19, 2003, 0 h 50 m UT, 17.3 S, 197.3 W) with strong quasi-regular amplitude and phase variations. The refractive attenuations of the CHAMP RO signals $X_a$ and $X_p$ found from the intensity and eikonal data are shown in Fig. 2 (left panel) as functions of the RO ray perigee altitude $h$. The eikonal acceleration $a$ has been estimated by the double differentiation of a second-power least-square polynomial over a sliding time interval $\Delta t = 0.5$ s. This time interval approximately corresponds to the vertical size of the Fresnel zone of $\sim$1 km since the vertical component of the radio ray was $\sim$2.1 km/s. The refractive attenuation $X_p$ is derived from the evaluated magnitude $a$ using (4), and the $m$ value is obtained from the orbital data. The refractive attenuation $X_a$ is derived from the RO amplitude data by a sliding least-square polynomial having the same power with averaging in the same time interval of 0.5 s. In the altitude ranges of 42–46 and 98–106 km, the refractive attenuations variations $X_a$ and $X_p$ are strongly connected and may be considered as coherent oscillations caused by sporadic layers (see left panel of Fig. 2). Using the Hilbert numerical transform, amplitudes $A_a$ and $A_p$ of analytical signals related to $X_a - 1$ and $X_p - 1$ have been computed and are shown in Fig. 2 (right panel). In the altitude range of 42–46 km, amplitudes $A_a$ and $A_p$ are nearly identical, but the magnitude of $A_a$ is about 1.5 times greater than that of $A_p$. Accordingly, a plasma layer is displaced from the RO ray perigee $T$ in the direction to satellite $G$ (see Fig. 1). A similar form of variations of the refractive attenuations $X_a - 1$ and $X_p - 1$ allows locating the detected ionospheric layer. Displacement $d$ corresponding to a plasma layer recorded at the 44-km altitude of the RO ray perigee is shown in Fig. 3 (left). Curves 1 and 2 in Fig. 3 (left) correspond to amplitudes $A_a$ and $A_p$. Curve 3 describes displacement $d$ found from amplitudes $A_a$ and $A_p$ using (18). The changes in $d$ are concentrated in the altitude range of 750–1150 km when functions $A_a$ and $A_p$ vary near their maximal values of 0.46 and 0.69 in the ranges of $0.4 \leq A_p \leq 0.46$ and $0.5 \leq A_a \leq 0.69$, respectively. The statistical error in the determination of ratio $A_a - A_p/A_p$ in (18) is minimal when $A_p$ is maximal. Point $a$ in Fig. 3 (left panel) marks the maximum value of $A_p$, and points $b$ and $c$ denote the corresponding values $A_a = 0.67$ and $d = 940$ km, respectively; the plasma layer is displaced from the RO ray perigee $T$ in the direction of the navigational

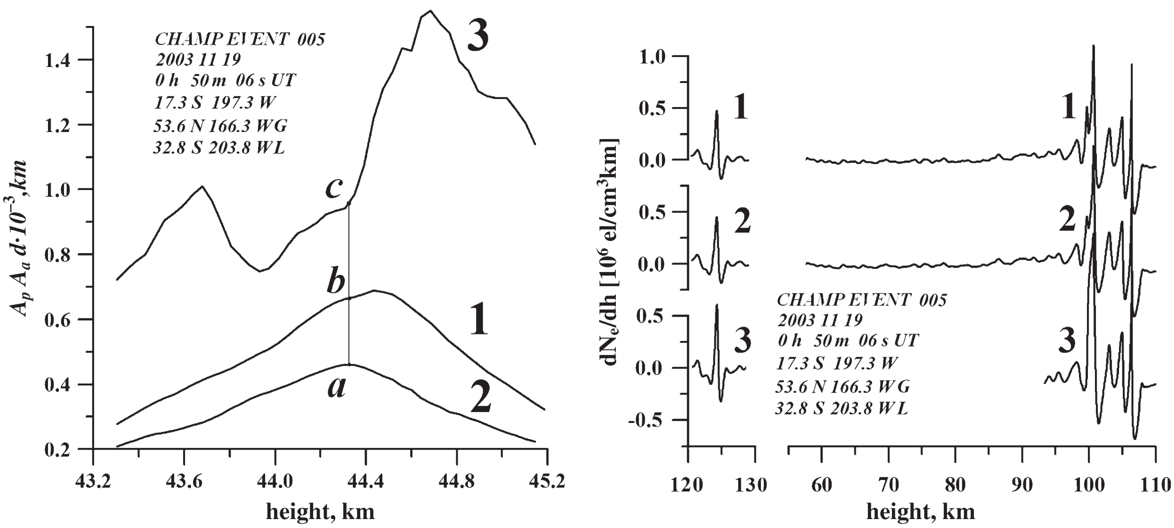


Fig. 3. (Left) Evaluation of the plasma layer displacement $d$ from the RO perigee. (Right) Results of the restoration of the vertical gradients of the electron density.

satellite $G$ (see Fig. 1). If the relative error in the measurements of $A_p$ is 5%, then, according to Fig. 3 (left), the accuracy in the estimation of $d$ is about $\pm 120$ km. The inclination of a plasma layer to a local horizontal direction calculated using (19) is approximately equal to $\delta = 10.4^\circ \pm 0.2^\circ$. The vertical gradient $dN_e/dh$ of the electron density distribution $N_e(h)$ for the given RO event is shown in Fig. 3 (right). Curves 1 and 2 correspond to the vertical gradient $dN_e/dh$ retrieved using (20) and (22), respectively. Curve 3 is related to the vertical gradient $dN_e/dh$ retrieved using the refractive attenuation $X_a$ and formula (22). The real altitude of the ionospheric layers is indicated on the horizontal axis in Fig. 3 (right). Two ionospheric layers are seen (curves 1, 2, and 3 in Fig. 3, right). The first layer is located on line $GT$ at the 120- to 130-km altitudes at a distance of $\sim$950 km from point $T$. The second layer is located near the RO perigee at the 98- to 108-km altitudes [see Figs. 2 and 3 (right)]. From the comparison of the refractive variations $X_a$ and $X_p$ (see left of Fig. 2) and the vertical gradients of the electron content (see right of Fig. 3), the width of the sporadic $E$-layers is nearly equal to the altitude interval of the amplitude variations of RO signals. From Fig. 3 (right), the variations of the vertical gradient of the electron density are concentrated in interval $-1.1 \cdot 10^6$ el/cm$^3$km $< dN(h)/dh <$ $1.1 \cdot 10^6$ el/cm$^3$km. These magnitudes of $N(h)$ are typical for intensified sporadic $E$-layers [29]. The height interval of the amplitude variations is nearly equal to the height interval of the variations in the electron density and its gradient.

The second example of the identification and the location of the sporadic plasma layer in the lower ionosphere is shown in Fig. 4 for CHAMP RO event 211 (July 04, 2003, 10 h 54 m LT, 2.1 N, 145.6 W) with intensive sporadic $E$-layers. The refractive attenuations $X_a$ and $X_p$ of the CHAMP RO signals at $f_1$ obtained from the intensity and eikonal data are shown in Fig. 4(a) as functions of the RO ray perigee altitude $h$. The refractive attenuations variations $X_a$ and $X_p$ are strongly correlated and can be considered as coherent oscillations caused by a single sporadic $E$-layer. As shown in Fig. 4(b), magnitude $A_a$ is about 1.3 times greater than $A_p$. This means that a corresponding plasma layer is displaced from the RO ray perigee $T$ in the direction to satellite $G$ (see Fig. 1). Curves 1, 2, and 3 in Fig. 4(c) are displacement $d$ (its values are marked at the left vertical axis), the layer slope $\delta$ (in degrees; right vertical axis), and correction $\Delta h$, respectively. Curves 1, 2, and 3 in Fig. 4(d) are amplitudes $A_a$ and $A_p$ and the corrected height $h'$ of the plasma layer maximum on the RO ray perigee altitude $h$, respectively. The changes in $d$, $\Delta h$, and $\delta$ are concentrated in the ranges of 240–400 and 5–15 km, and $2.2^\circ \ldots 3.2^\circ$ when the altitude of the RO ray perigee changes in the range of 109.6–110.4 km. From these changes, the average values of $d$, $\Delta h$, and $\delta$ are determined, i.e., $d = 350$ km $\pm$ 50 km; $\Delta h =$ 10 km $\pm$ 5 km, and $\delta = 3.1^\circ \pm 0.3^\circ$. It is concluded that the detected sporadic layer is displaced from the RO ray perigee by 350 km in the direction to the GPS satellite and the altitude of which is 10 km greater than the height of point $T$. The height distribution of the electron density $N_e(h')$ and its altitude gradient $dN_e(h')/dh'$ recalculated from the modernized Abel inversion (22) are shown in Fig. 4(e) and (f). Note that function $N_e(h')$ represents the sporadic $E$-layer contribution with approximation $N(t_x, p_0) = 0$. This suggests that the aforementioned calculation reflects the high-frequency part $N_e(h')$ and with the magnitude of the vertical spatial periods below 10 km. The maximal value of the electron density is located at the height of 119.2 km [see Fig. 4(e)]. The maximal gradient of the electron content $\sim 1.4 \cdot 10^6$[el/cm$^3$km] is observed at the altitude of 119.0 km [see Fig. 4(f)]. The altitude dependent quantity $N_e(h')$ demonstrates the wavelike structure that is possibly related to the wind shears in the vertical distribution of horizontal wind in the neutral gas [46].

The introduced method appears to have a considerable potential to resolve the uncertainty between parts $GT$ and $LT$ of the ray trajectory and determine the location of inclined layers. This method accurately indicates the locations of the maximal values and the direction of the gradient of the electron density including the distance, the altitude, and the slope. According to the existing theory, the maximum of the electron content in sporadic $E$-layers is usually connected with the influence

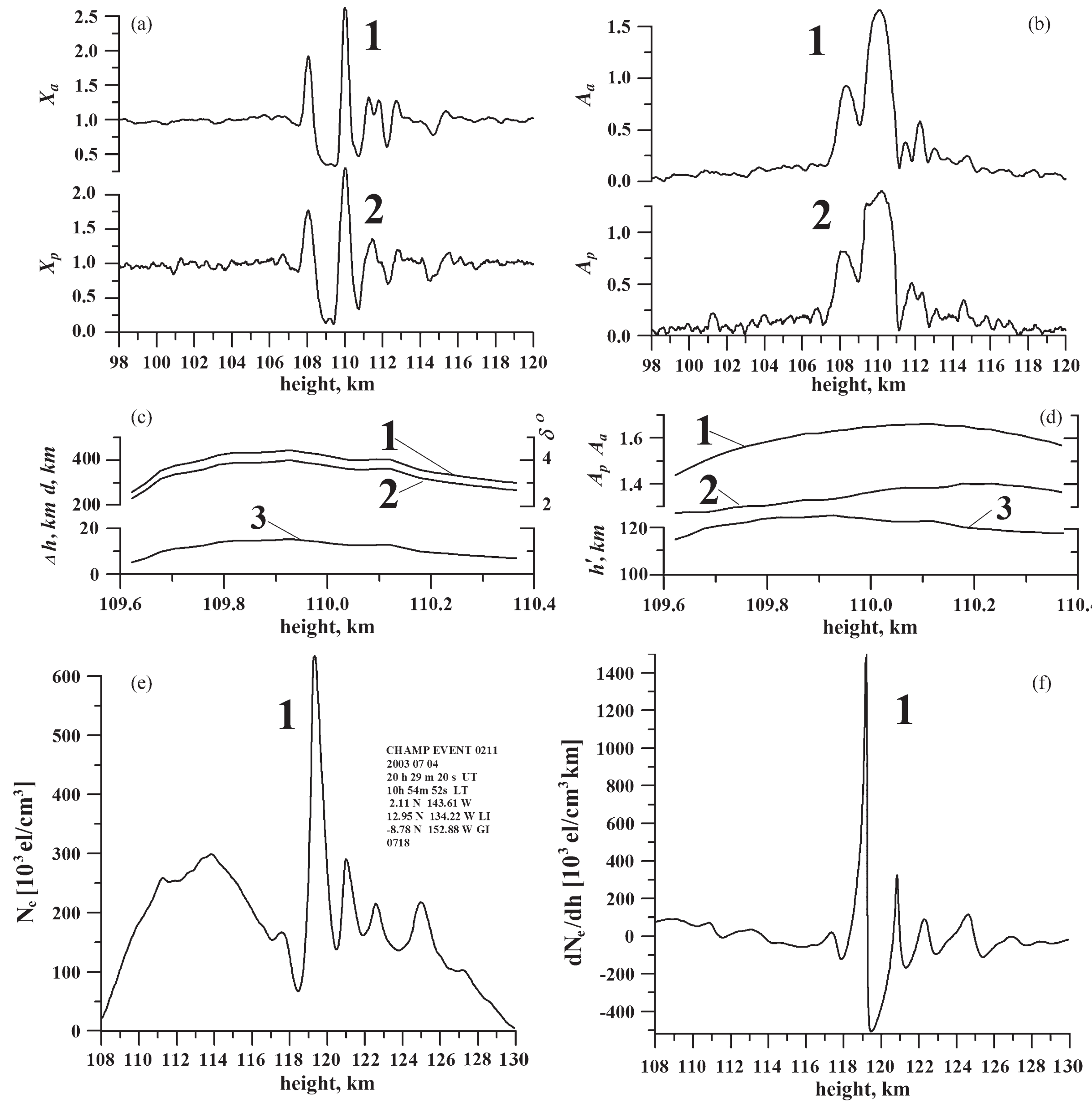


Fig. 4. (a)–(d) Identification and location of a layer in the lower ionosphere. (e) Distribution of the electron density in the identified sporadic $E_s$ layer. (f) Distribution of the gradient of electron density.

of the wind shear [29]. Therefore, the RO method is capable of locating the wind shear in the lower ionosphere. The gradient of the electron content can correspond to the wave fronts of different kinds of wave influencing on the ionospheric plasma distribution [46]. In the case of the internal GWs, the inclination of the wave vector to the vertical direction can be used to find the angular frequency of the GW [40]. Therefore, the introduced criterion and technique extended the applicable domain of the RO method. The additional validation of this method through analyzing the CHAMP data and comparison with ground-based ionosonde information is the task for the future work.

## IV. Conclusion

The analytic technique is a new method for locating the inclined layered structures (including sporadic $E_s$ layers) in the ionosphere. The location of the ionospheric layers including their altitude, displacement from the RO ray perigee, and slope relative to the horizontal direction can be determined using the introduced criterion that compares the refractive attenuations found from the RO amplitude and phase data for both theoretical and experimental analyses of the RO signals. Depending on the sign of the refractive attenuations, the displacement of a plasma layer from the RO ray perigee should be positive (in the direction to a GPS satellite and vice versa). The magnitude of the displacement can be found from a ratio of the refractive attenuation's difference to the magnitude of the refractive attenuation from the RO phase data. The altitude and the slope of a plasma layer can be found from the known value of its displacement. Therefore, the standard estimation of a layer's altitude as a height of the RO ray perigee should be revised due to the underestimation of the altitude of inclined plasma structures in the lower ionosphere. The accuracy of the current radio-holographic backpropagation method depends on the form of the Green function used for the backpropagation. If the Green function corresponding to the propagation in the free space is used, then the inaccuracy of the backpropagation method is proportional to the bending angle. The analytic technique based on the locality principle is simpler and more precise than the backpropagation method. By the use of the introduced criterion, the RO method is capable of locating and determining the direction and the magnitude of the gradient of the electron density in the lower ionosphere.

The gradient of the electron content indicates the direction of the different kinds of wave fronts in the ionosphere. In the particular case of the internal GWs, the inclination of the wave vector to the vertical direction can be used to find the angular frequency and the parameters of the GW. Therefore, the introduced criterion and technique extended the applicable domain of the RO method to remote sensing internal waves in the lower ionosphere. This conclusion has a general importance for the planetary and terrestrial RO experiments in a broad range of frequencies.

## Acknowledgment

The authors would like to thank GeoForschungsZentrum (GFZ) Potsdam for access to the CHAllenge Minisatellite Payload (CHAMP) radio occultation data.

## References


[1] A. Rius, G. Ruffini, and A. Romeo, “Analysis of ionospheric electron density distribution from GPS/MET occultations,” *IEEE Trans. Geosci. Remote Sens.*, vol. 36, no. 2, pp. 383–394, Mar. 1998.

[2] G. A. Hajj and L. J. Romans, “Ionospheric electron density profiles obtained with the Global Positioning System: Results from GPS/MET experiment,” *Radio Sci.*, vol. 33, no. 1, pp. 175–190, 1998.

[3] K. Igarashi, A. Pavelyev, K. Hocke, D. Pavelyev, and J. Wickert, “Observation of wave structures in the upper atmosphere by means of radio holographic analysis of the radio occultation data,” *Adv. Space Res.*, vol. 27, no. 6/7, pp. 1321–1326, 2001.

[4] K. Igarashi, A. G. Pavelyev, J. Wickert, K. Hocke, and D. A. Pavelyev, “Application of radio holographic method for observation of altitude variations of the electron density in the mesophere/lower thermosphere using GPS/MET radio occultation data,” *J. Atmos. Solar-Terrestrial Phys.*, vol. 64, no. 8–11, pp. 959–969, May 2002.

[5] J. Wickert, C. Reigber, G. Beyerle, R. Konig, C. Marquardt, T. Schmidt, L. Grunwaldt, R. Galas, T. K. Meehan, W. G. Melbourne, and K. Hocke, “Atmosphere sounding by GPS radio occultation: First results from CHAMP,” *Geophys. Res. Lett.*, vol. 28, no. 9, pp. 3263–3266, 2001.

[6] J. Wickert, A. G. Pavelyev, Y. A. Liou, T. Schmidt, C. Reigber, K. Igarashi, A. A. Pavelyev, and S. Matyugov, “Amplitude scintillations in GPS signals as a possible indicator of ionospheric structures,” *Geophys. Res. Lett.*, vol. 31, no. 15, pp. L24801-1–L24801-4, 2004.

[7] A. S. Jensen, M. Lohmann, H.-H. Benzon, and A. S. Nielsen, “Full spectrum inversion of radio occultation signals,” *Radio Sci.*, vol. 38, no. 3, pp. 1040–1054, 2003.

[8] M. E. Gorbunov and K. B. Lauritsen, “Analysis of wave fields by Fourier integral operators and its application for radio occultations,” *Radio Sci.*, vol. 39, no. 4, pp. RS4010-1–RS4010-15, 2004.

[9] M. E. Gorbunov and G. Kirchengast, “Processing X/K band radio occultation data in presence of turbulence,” *Radio Sci.*, vol. 40, no. 6, pp. RS6001-1–RS6001-11, 2005.

[10] M. E. Gorbunov, A. S. Gurvich, and A. V. Shmakov, “Back-propagation and radio-holographic methods for investigation of sporadic ionospheric $E$-layers from Microlab-1 data,” *Int. J. Remote Sens.*, vol. 23, no. 4, pp. 675–685, 2002.

[11] M. E. Gorbunov, K. B. Lauritsen, and S. S. Leroy, “Application of Wigner distribution function for analysis of radio occultations,” *Radio Sci.*, vol. 45, pp. RS6011-1–RS6011-11, 2010.

[12] D. L. Wu, C. O. Ao, G. A. Hajj, M. de la Torre Juarez, and A. J. Mannucci, “Sporadic E morphology from GPS-CHAMP radio occultation,” *J. Geophys. Res.*, vol. 110, no. A1, pp. A01306-1–A01306-18, 2005.

[13] A. G. Pavelyev, Y. A. Liou, C. Y. Huang, C. Reigber, J. Wickert, K. Igarashi, and K. Hocke, “Radio holographic method for the study of the ionosphere, atmosphere and terrestrial surface using GPS occultation signals,” *GPS Solut.*, vol. 6, no. 2, pp. 101–108, 2002.

[14] A. G. Pavelyev, Y. A. Liou, and J. Wickert, “Diffractive vector and scalar integrals for bistatic radio- holographic remote sensing,” *Radio Sci.*, vol. 39, no. 4, pp. RS4011-1–RS4011-16, 2004.

[15] A. G. Pavelyev, Y. A. Liou, J. Wickert, T. Schmidt, A. A. Pavelyev, and S. F. Liu, “Effects of the ionosphere and solar activity on radio occultation signals: Application to CHAllenging Minisatellite Payload satellite observations,” *J. Geophys. Res.*, vol. 112, no. A6, pp. A06326-1–A06326-14, 2007.

[16] A. G. Pavelyev, Y. A. Liou, J. Wickert, A. L. Gavrik, and C. C. Lee, “Eikonal acceleration technique for studying of the Earth and planetary atmospheres by radio occultation method,” *Geophys. Res. Lett.*, vol. 36, no. L21, pp. L21807-1–L21807-5, 2009.

[17] A. G. Pavelyev, K. Zhang, C. S. Wang, Y. Kuleshov, Y. A. Liou, and J. Wickert, “Identification of inclined ionospheric layers using analysis of GPS occultation data,” *IEEE Trans. Geosci. Remote Sens.*, vol. 49, pt. 2, no. 6, pp. 2374–2384, Jun. 2011.

[18] Y. A. Liou, A. G. Pavelyev, C. Y. Huang, K. Igarashi, and K. Hocke, “Simultaneous observation of the vertical gradients of refractivity in the atmosphere and electron density in the lower ionosphere by radio occultation amplitude method,” *Geophys. Res. Lett.*, vol. 29, no. 20, pp. 1937–1940, 2002.

[19] Y. A. Liou, A. G. Pavelyev, C. Y. Huang, K. Igarashi, K. Hocke, and S. K. Yan, “Analytic method for observation of the GW using RO data,” *Geophys. Res. Lett.*, vol. 30, no. 21, pp. 2021–2025, 2003.

[20] Y. A. Liou, A. G. Pavelyev, A. A. Pavelyev, J. Wickert, and T. Schmidt, “Analysis of atmospheric and ionospheric structures using the GPS/MET and CHAMP radio occultation data base: A methodological review,” *GPS Solut.*, vol. 9, no. 2, pp. 122–143, Jun. 2005.

[21] Y. A. Liou, A. G. Pavelyev, S. F. Liu, A. A. Pavelyev, N. Yen, C. Y. Huang, and C. J. Fong, “FORMOSAT-3/COSMIC GPS radio occultation mission: Preliminary results,” *IEEE Trans. Geosci. Remote Sens.*, vol. 45, no. 11, pp. 3813–3826, Nov. 2007.

[22] Y. A. Liou, A. G. Pavelyev, S. S. Matyugov, O. I. Yakovlev, and J. Wickert, *Radio Occultation Method For Remote Sensing of the Atmosphere and Ionosphere*. Vukovar, Croatia: InTech, p. 170.

[23] C. Arras, J. Wickert, C. Jacobi, S. Heise, G. Beyerle, and T. Schmidt, “A global climatology of ionospheric irregularities derived from GPS radio occultation,” *Geophys. Res. Lett.*, vol. 35, no. L14, pp. L14809-1–L14809-4, 2008.

[24] C. Arras, C. Jacobi, and J. Wickert, “Semidiurnal tidal signature in sporadic E occurrence rates derived from GPS radio occultation measurements at higher midlatitudes,” *Ann. Geophys.*, vol. 27, no. 6, pp. 2555–2563, 2009.

[25] C. Arras, C. Jacobi, J. Wickert, S. Heise, and T. Schmidt, “Sporadic E signatures revealed from multi-satellite radio occultation measurements,” *Adv. Radio Sci.*, vol. 8, no. CHJ, pp. 225–230, 2010.

[26] N. Jakowski, R. Leitinger, and M. Angling, “Radio occultation techniques for probing the ionosphere,” *Ann. Geophys.*, vol. 47, no. 2/3, pp. 1049–1066, 2004.

[27] V. E. Kunitsyn and E. D. Tereshchenko, *Ionospheric Tomography*. Berlin, Germany: Springer-Verlag, 2003.

[28] M. C. Kelley, V. K. Wong, G. A. Hajj, and A. J. Mannucci, “On measuring the off-equatorial conductivity before and during convective ionospheric storms,” *Geophys. Res. Lett.*, vol. 31, no. L17, pp. L17805-1–L17805-3, 2004.

[29] M. C. Kelley and A. Heelis, *The Earth’s Ionosphere: Plasma Physics and Electrodynamics,* 2nd ed. New York: Academic, 2009.

[30] A. G. Pavelyev, Y. A. Liou, J. Wickert, K. Zhang, C. S. Wang, and Y. Kuleshov, “Analytical model of electromagnetic waves propagation and location of inclined plasma layers using occultation data,” *Prog. Electromagn. Res.*, vol. 106, pp. 177–202, 2010. doi: 10.2528/PIER10042707.

[31] A. G. Pavelyev, Y. A. Liou, J. Wickert, T. Schmidt, A. A. Pavelyev, and S. S. Matyugov, “Phase acceleration: A new important parameter in GPS occultation technology,” *GPS Solut.*, vol. 14, no. 1, pp. 3–11, 2010.

[32] A. G. Pavelyev, Y. A. Liou, K. Zhang, C. S. Wang, J. Wickert, T. Schmidt, V. N. Gubenko, A. A. Pavelyev, and Y. Kuleshov, “Identification and localization of layers in the ionosphere using the eikonal and amplitude of radio occultation signals,” *Atmos. Meas. Tech.*, vol. 4, no. 2, pp. 1465–1492, 2012.

[33] J. Whitehead, “The formation of the sporadic-E layer in the temperate zones,” *J. Atmos. Terr. Phys.*, vol. 20, no. 1, pp. 49–58, Feb. 1961.

[34] J. M. C. Plane, “Atmospheric chemistry of meteoric metals,” *Chem. Rev.*, vol. 103, no. 12, pp. 4963–4984, Dec. 2003.

[35] C. Haldoupis, D. Pancheva, W. Singer, C. Meek, and J. Mac-Dougall, “An explanation for the seasonal dependence of midlatitude sporadic E layers,” *J. Geophys. Res.*, vol. 112, no. A6, pp. A06315-1–A06315-7, 2007.

[36] W. G. Melbourne, E. S. Davis, C. B. Duncan, G. A. Hajj, K. R. Hardy, E. R. Kursinski, T. Meehan, K. L. E. Young, and T. P. Yunck, “The application of spaceborne GPS to atmospheric limb sounding and global change monitoring,” Jet Propul. Lab., Pasadena, CA, 1994.

[37] W. G. Melbourne, *Radio Occultations Using Earth Satellites: A Wave Theory Treatment, Monograph 6, Deep Space Communications and Navigation Series*, J. H. Yuen, Ed. Pasadena, CA: Jet Propul. Lab, 2004.

[38] M. E. Gorbunov, “Ionospheric correction and statistical optimization of radio occultation data,” *Radio Sci.*, vol. 37, no. 5, pp. 1084–1092, 2002.

[39] V. V. Vorob’ev and T. G. Krasilnikova, “Estimation of accuracy of the atmosphere refractive index recovery from Doppler shift measurements at frequencies used in the NAVSTAR system,” *Phys. Atmos. Ocean.*, vol. 29, no. 5, pp. 602–609, 1994.

[40] V. N. Gubenko, A. G. Pavelyev, and V. E. Andreev, “Identification of wave origin of temperature fluctuations and determination of the intrinsic frequency of internal gravity waves in the Earth’s stratosphere derived from radio occultation data,” *J. Geophys. Res.*, vol. 113, no. D8, p. D08109, 2008.

[41] V. V. Vorob’ev, A. S. Gurvich, V. Kan, S. V. Sokolovskiy, O. V. Fedorova, and A. V. Shmakov, “The structure of the ionosphere from the GPS-“Microlab-1” radio occultation data: Preliminary results,” *Cosmic Res.*, no. 4, pp. 74–83, 1997.

[42] S. V. Sokolovskiy, W. Schreiner, C. Rocken, and D. Hunt, “Detection of high-altitude ionospheric irregularities with GPS/MET,” *Geophys. Res. Lett.*, vol. 29, no. 3, pp. 621–625, 2002.

[43] Y. A. Liou and A. G. Pavelyev, “Simultaneous observations of radio wave phase and intensity variations for locating the plasma layers in the ionosphere,” *Geophys. Res. Lett.*, vol. 33, no. 23, pp. L23102-1–L23102-5, 2006.

[44] K. Hocke, “Inversion of GPS meteorology data,” *Ann. Geophys.*, vol. 15, no. 4, pp. 143–152, Apr. 1997.

[45] A. G. Pavelyev and A. I. Kucherjavenkov, “Refractive attenuation in the planetary atmospheres,” *Radio Eng. Electron. Phys.*, vol. 23, no. 7, pp. 13–19, Jul. 1978.

[46] A. G. Pavelyev, T. Tsuda, K. Igarashi, Y. A. Liou, and K. Hocke, “Wave structures in the electron density profile in the ionospheric $D$ and $E$-layers observed by radio holography analysis of the GPS/MET radio occultation data,” *J. Atmos. Solar-Terr. Phys.*, vol. 65, no. 1, pp. 59–70, 2003.

**Alexander G. Pavelyev** received the B.Sc. and M.Sc. degrees from Gorky State University, Gorky, Russia, and the Ph.D. degree in radio physics from the Academy of Sciences of the U.S.S.R., Moscow, Russia, in 1969.

He was a Senior Researcher (Assistant Professor) in 1977 and a Leading Researcher in early 1987. He was Senior Scientist granted by Telecommunication Advanced Organization (TAO) of Japan in late 1999/early 2000 and Senior Research Scientist granted by the Science and Technology Agency (STA) Fellowship Program in late 2000 with Communication Research Laboratory (CRL), Japan. Since June 2000, he has been the Head of the Laboratory of Radio Wave Propagation in Space, Kotelnikov Institute of Radio Engineering and Electronics (Fryazino branch), Russian Academy of Sciences (FIRE RAS). In early 2001, he was a Visiting Professor with Radio Science Center for Space and Atmosphere (RASC) Kyoto University, Kyoto, Japan. He was a Visiting Professor with the Centre for Space and Remote Sensing Research National Central University, Taoyuan, Taiwan (2002–2006 and 2009). From April to May 2010, He was also a Visiting Professor with the Satellite Positioning for Atmosphere, Climate and Environment Research Centre, Royal Melbourne Institute of Technology, Melbourne, Australia.

**Kefei Zhang** received the B.Sc. and M.Sc. degrees in Geodesy from Wuhan University (former Wuhan Technical University of Surveying and Mapping) and a Ph.D. in Geodesy from Curtin University of Technology, Australia.

Since late 1999, he has been with the Royal Melbourne Institute of Technology University, Melbourne, Australia, where he is currently a Professor, the Founder, and the Director of the Satellite Positioning for Atmosphere, Climate and Environment Research Centre. He is a coholder of eight international patents. He has authored over 250 peer-reviewed papers in these fields since 1990 and has attracted in excess of 12 million dollars in funding from the Australian Research Council, government, research, and industry sectors. He is a regular reviewer of various national and international funding agencies and journals, a member of journal editorial boards, and a frequent speaker/guest at various international events. He is currently the Chief Scientist of the multimillion-dollar prestigious Australia Space Research Program Platform Technologies project and leads an international team that comprises a number of international leading scientists in the areas of satellite positioning, space tracking, atmosphere, and climate-change research to develop innovation solutions using cutting-edge space technologies. His main areas of expertise are in satellite positioning, navigation, and geodesy. His current research is primarily involved in algorithm development and innovative applications of Global Navigation Satellite System (GNSS)/Global Positioning System technologies for high-accuracy positioning, atmospheric studies (e.g., for space weather, space debris surveillance and collision warning, Square Kilometer Array project (SKA), climate change, weather and environment, and ionosphere), space tracking, satellite orbit determination, and people mobility and object tracking.

**Yuei-An Liou** (S’91–M’96–SM’01) received the B.Sc. degree in electrical engineering (EE) from the National Sun Yat-sen University, Kaohsiung, Taiwan, in 1987 and the M.Eng. degree in EE, the M.Sc. degree in atmospheric and space sciences, and the Ph.D. degree in EE and atmospheric, oceanic, and space sciences from the University of Michigan, Ann Arbor, in 1992, 1994, and 1996, respectively.

He is currently with the Center for Space and Remote Sensing Research, National Central University, Chung-Li, Taiwan. He is a Principal Investigator on many research projects sponsored by the National Science Council (NSC), the Council of Agriculture, the National Space Organization (NSPO), the Civil Aeronautics Administration, the Minister of Interior, the Water Conservancy Agency of Taiwan, and the Office of Naval Research of USA. He has authored over 60 journal and 130 international conference papers.

Dr. Liou serves as a leading Guest Editor for the IEEE TRANSACTIONS ON GEOSCIENCE AND REMOTE SENSING special issue “Meteorology, Climate, Ionosphere, Geodesy, and Reflections from the Ocean Surfaces: Studies by Radio Occultation Methods.” He was a recipient of the Annual Research Awards from the NSC in 1998, 1999, and 2000; the First Class Research Awards from the NSC in 2004, 2005, and 2006; and the National Central University (NCU) Outstanding Research Awards in 2004 and 2006, respectively. He was awarded the “Contribution Award to FORMOSAT-3 National Space Mission” by NSPO in 2006. He is a member of the American Geophysical Union, the American Meteorological Society, and the International Association of Hydrological Sciences. He is an Honorary Life Member of the Korean Society of Remote Sensing.

**Alexey A. Pavelyev** was born in Russia in 1986. He received the B.S. and M.S. degrees from Moscow Chemical Technology University, Moscow, Russia.

He is currently a Junior Scientist with the Kotelnikov Institute of Radio Engineering and Electronics, Russian Academy of Sciences, Moscow. He is interested in developing automatic processing systems for radio occultation data and the application of radio occultation data in atmospheric and climate research.

**Chuan-Sheng Wang** received the B.Sc. and M.Sc. degrees from the National Chiao Tung University, Hsinchu, Taiwan, in 1998 and 2000, respectively, and the Ph.D. degree in space sciences from the National Central University, Taoyuan, Taiwan, in 2009.

He is currently a Research Fellow with the School of Mathematical and Geospatial Sciences, Royal Melbourne Institute of Technology University, Melbourne, Australia. He is also currently with the National Taipei University, Taipei, Taiwan. His research interests include precise Global Positioning System positioning and meteorology.

**Jens Wickert** was born in 1963. He received the Ph.D. degree in geophysics/meteorology from Karl-Franzens-University Graz, Graz, Austria, in 2002.

He worked for several years in atmospheric research for the German Weather Service, Alfred-Wegener-Institute for Polar and Marine Research, and German Aerospace Center. Since 1999, he has been with GeoForschungsZentrum Potsdam, Potsdam, Germany, and he is currently the Acting Head of Section 1.1 GPS/Galileo Earth Observation. He is responsible for various GNSS-related research projects. He is the author and coauthor of numerous papers related to GNSS remote sensing in peer-reviewed journals.

**Torsten Schmidt** received the M.S. degree in meteorology from Humboldt University of Berlin, Berlin, Germany, in 1989 and the Ph.D. degree in atmospheric physics from the University of Bremen, Bremen, Germany, in 1999.

Since 1999, he has been with the section "GPS/Galileo Earth Observation," GeoForschungsZentrum (GFZ), Potsdam, Germany. He has authored or reviewed several leading scientific journals. He is interested in developing automatic processing systems for radio occultation data and the application of radio occultation data in atmospheric and climate research.

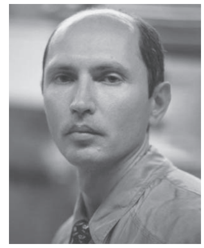

**Yuriy Kuleshov** received the B.Sc. degree in electronic engineering from the Institute of Radio Engineering, Kharkov, Ukraine, in 1981 and the Ph.D. degree in physics and mathematics from the Institute of Radio Physics and Electronics (IRPE), Academy of Sciences, Kharkov, Ukraine, in 1991.

From 1981 to 1994, he worked with IRPE as a Researcher on the design of the satellite and aircraft microwave remote sensing systems for obtaining environmental information, including the first Soviet space radar of the "Cosmos/Ocean" satellite series, and the aircraft-laboratory multifrequency microwave remote sensing system. He also worked on the development of new methods of deriving, processing, and interpreting environmental information for marine environment (sea ice and iceberg observations, oil spill detection, near-surface wind speed retrieval, and investigations of tropical cyclones) and terrestrial environment (freshwater ice, glaciers, and vegetation monitoring). Since 1995, he has been the Project Leader at the Australian Bureau of Meteorology (BoM) for the international initiative on "Climate change and tropical cyclones in the Southern Hemisphere: Development of the tropical cyclone archive, climatology and seasonal prediction for the region." He also works on the development of new methods of satellite remote sensing (GPS radio occultation and GPS reflectometry) for applications to climatology and oceanography. He is currently the Australian Team Leader on the Seasonal Climate Prediction Project, Pacific Adaptation Strategy Assistance Program (PASAP) at BoM and an Adjunct Professor with the School of Mathematical and Geospatial Sciences, Royal Melbourne Institute of Technology University, Melbourne, Australia. Dr. Kuleshov is the Australian representative of the World Meteorological Organization Commission for Climatology Open Panels of Experts on Climate Monitoring and Assessment. He also represents the BoM for the Standards Australia, providing advice and expert opinion on climate science relevant to the committees "Lightning protection" and "Wind actions" activities.